Vol. 13: 115–123, 1999 | CLIMATE RESEARCH Clim Res | Published October 26

Surface CO_2 exchange in an intensively managed peat pasture

B. O. M. Dirks[1,*], A. Hensen[2], J. Goudriaan[1]

[1]Wageningen Agricultural University, Dept of Theoretical Production Ecology, PO Box 430, 6700 AK Wageningen, The Netherlands

[2]Netherlands Energy Research Foundation, PO Box 1, 1755 ZG Petten, The Netherlands

ABSTRACT: Aerodynamic measurements of CO_2 *(F)* and latent heat *(λE)* exchange were made in an intensively managed peat pasture during 2 consecutive years; the fetch was approximately 1.5 km. Surface conductance *(g_s)* was calculated from the Penman-Monteith equation. *F* was split into a respiratory CO_2 flux *(F_r)* and an assimilatory CO_2 flux *(F_a)*. F_r was non-linearly related to air temperature *(T_a)*, revealing a distinct seasonal pattern in its value normalized to T_a. F_a was hyperbolically related to short-wave irradiance, the seasonal pattern of its maximum value compared to that of normalized F_r. T_a proved to be a major factor: F_a tended to maintain a positive response to T_a over much of the actual T_a range. Aerial vapour pressure deficit *(D)* was generally too low (<1 kPa) to have an effect on F_a.

KEY WORDS: Aerodynamic technique · CO_2 exchange · Assimilatory flux · Respiratory flux · Surface conductance · Pasture · Grassland

1. INTRODUCTION

General circulation models indicate that the atmospheric CO_2 concentration is an important climatic factor (Sellers et al. 1986, Manabe et al. 1991). Atmospheric CO_2 constitutes a small but important interface between most large pools of the global C cycle (Sundquist 1993) with a relatively small time coefficient. Annual oscillations in the atmospheric CO_2 concentration—reaching an amplitude of up to 20 µmol mol^{-1} in the Northern Hemisphere—illustrate seasonal shifts in terrestrial biospheric respiratory and assimilatory activity (Fung et al. 1983, 1987, Kaduk & Heimann 1996, Nemry et al. 1996). Long-term trends in these oscillations suggest a gradually increasing amplitude and a progressively earlier draw-down in spring (Cleveland et al. 1983, Bacastow et al. 1985). These changes may well reflect the interaction between a changing atmospheric CO_2 concentration, climate and biospheric activity (Kohlmaier et al. 1989, Keeling et al. 1996).

On the balance sheet of global C flows, a net biospheric CO_2 uptake (Tans et al. 1990, Goudriaan 1994, Hudson et al. 1994, King et al. 1995) is thought to mitigate anthropogenic emissions (Sundquist 1993, Houghton et al. 1996). However, global sinks and sources of CO_2 show large differences in their spatial and temporal arrangement (Box 1988). Measurements of atmospheric-biospheric CO_2 exchange have been made in many ecosystems (Verma & Rosenberg 1976, Baldocchi et al. 1981, Anderson et al. 1984, Anderson & Verma 1986, Dunin et al. 1989, McGinn & King 1990, Baldocchi 1994). Few authors report periods that extend beyond the growing season, as the measurements are often done in a crop physiological context rather than for the characterization of biospheric activity. Long-term measurement of CO_2 exchange in an undisturbed Amazonian rainforest and subsequent analysis in relation to environmental factors revealed a yearly net CO_2 uptake (Fan et al. 1990, Grace et al. 1995).

Grasslands constitute an important component of the biospheric C storage (Wolf & Janssen 1991). This paper reports on micrometeorological CO_2 flux measurements in intensively managed peat pasture made dur-

*E-mail: bjorn.dirks@altavista.net

ing 2 consecutive years. Firstly, the analysis separates the instantaneous flux in respiratory and assimilatory CO_2 flux components. Secondly, the analysis investigates the relationships between on the one hand the CO_2 flux components and on the other hand irradiance, temperature and vapour pressure deficit, and assesses their seasonal course.

2. MATERIALS AND METHODS

2.1. Experimental site. Measurements were made at the experimental site of the Royal Netherlands Meteorological Institute (KNMI) near Cabauw in The Netherlands (51° 58' N, 4° 55' E). It was surrounded by pasture, orchards, minor roads and a built-up area. The soil consisted of a 0.6 to 0.8 m thick layer of alluvial clay on top of a massive peat layer. The land was composed of long strips alternated by waterways (every 50 m, approximately 5% of the total surface). The vertical distance between land and waterway surface amounted to approximately 0.8 m. The pasture predominantly consisted of *Lolium perenne* and was used for intensive dairy farming (2.5 head of cattle ha^{-1}), with mixed grazing and mowing.

Only measurements made while the wind direction was between 195° and 250° were analysed. In this range the fetch almost exclusively consisted of pasture over a distance of approximately 2 km. To assess CO_2 sources and C flows other than vegetative, a brief survey was made in April 1993 of the 5 dairy farms that constituted most of the land in the 195° to250° range.

2.2. Flux measurements. The micrometeorological CO_2 and latent heat flux λE exchange measurements (Hensen et al. 1997) covered most of the periods March 1993 up to February 1994 ('1993'), and March 1994 up to February 1995 ('1994'). In applying the aerodynamic gradient technique, the Netherlands Energy Research Foundation (ECN) determined the CO_2 concentration profiles, whereas KNMI determined the profiles of the other variables.

Temperature measurements were obtained at 0.6, 2 and 5 m height. Thermocouples measured the direct differences between the successive levels (accuracy 0.05°C); at 0 m they were measured against a 0°C ice bath. Wind speed and direction were determined at 10 m height using a Gill propeller vane 8002dx, modified by KNMI (accuracy 1%). Air humidity followed from temperature and wet bulb temperature; the set-up of latter measurement was similar to that of temperature, but the sensor was kept wet using peristaltic pumps.

Air sampling for determination of the CO_2 concentration gradient was done at 1, 2 and 10 m height (Hensen et al. 1997). The air was transported through 50 m of polyethylene tubing, heated to 5°C above ambient to avoid condensation of water vapour. CO_2 concentrations were measured using a NDIR (Ultramat 5e, Siemens) with a N_2-filled reference cell. Before entering the measurement cell, the air was led through a humidifier and a Peltier cooling element maintaining dew point at 5°C. The monitor was calibrated daily using N_2 as zero gas; the span was calibrated using commercially available CO_2 standards which, in turn, had been calibrated against NOAA standards.

The different heights were sampled for 2 min: the monitor was flushed for 20 s and the CO_2 concentration was calculated from the measurements during the remaining 100 s. A full CO_2 profile was obtained every 8 min. The concentration data were clustered to 30 min averages, excluding measurements at a coefficient of drag <0.02 and during malfunctioning. High stability situations (with differences of up to 500 µmol mol^{-1} between 1 and 2 m height) were rejected. Errors in the calculation of the CO_2 flux (F) occur when the requirements for the gradient technique are not met. Inhomogeneities in terms of upwind obstacles can cause errors, but their frequency was low. The absence of local CO_2 sources avoided horizontal CO_2 gradients—a potential source of error. The effect of CO_2 storage below the sampling inlet was generally small, since a profile was measured every 8 min and the lower inlet was at 1 m height. The limited resolution of the monitor (0.5 µmol mol^{-1}) would have led to a 25% uncertainty in the calculated CO_2 fluxes if 1 profile would have been used. The 3 subsequent 8 min profiles in a 30 min average had a standard deviation of about 40%, depending on the meteorological conditions.

F (mg m^{-2} s^{-1}), λE (W m^{-2}), wind speed at 10 m height (u_{10}; m s^{-1}); air temperature at 0.6 m height (T_a; °C), and vapour pressure deficit at 0.6 m height ($D_{0.6}$; kPa) were considered. The fluxes were an average of the different states within the fetch of 1.5 km. The measurements were generally analysed at a monthly time scale. A distinction was made between daytime and nighttime measurements.

2.3. Meteorological measurements. Meteorological measurements and data processing were made by KNMI. Short-wave irradiance (0.3 to 3 µm) was measured using a Kipp CM11 pyranometer, ventilated to prevent condensation on the dome; for diffuse irradiance the pyranometer was equipped with a shadow band. Long-wave irradiance (3 to 50 µm) was measured using a ventilated Eppley radiometer. Measurement of net radiation (0.3 to 50 µm) was made by a Funk radiometer. Values for the following variables were reduced to 30 min averages (W m^{-2}): short-wave irradiance (R_s); outgoing long-wave irradiance (L_{out}).

2.4. Surface conductance. Surface conductance to water vapour transfer (g_s) was used for analysis of the F dynamics. g_s was calculated from the Penman-Mon-

teith equation (Monteith & Unsworth 1990). Use was made of λE, net radiation (R_n), u_{10}, $D_{0.6}$ and T_a. Aerodynamic conductance to water vapour transfer (g_a) was calculated as $(u_{0.6}/u_*^2 + 5.31u_*^{-2/3})^{-1}$ (Thom 1972, 1975, Verma et al. 1986, Monteith & Unsworth 1990, Lhomme 1991, Saugier & Katerji 1991), where u_* is the friction velocity. $u_{0.6}$ was calculated from the logarithmic wind profile, with $u_* = 0.141u_{10}$; zero plane displacement = 0.05 m. We assumed constant values for the soil heat flux (0 W m^{-2}), air pressure (101 kPa), psychrometer constant (γ; 0.066 kPa K^{-1}), latent heat of vaporization (2477 J g^{-1}), density of dry air (1246 g m^{-3}), and roughness length (0.03 m). g_s integrates leaf area and leaf characteristics (Mascart et al. 1991, Saugier & Katerji 1991, Kelliher et al. 1995).

For this analysis, situations with wet surfaces were excluded by only considering values at a λE and equilibrium latent heat flux (λE_{eq}) > 0 W m^{-2}. λE_{eq} is λE in a situation where g_a approaches 0; it equals $s \times R_n/(s + \gamma)$ (Jones 1992). s is the slope of the saturation vapour pressure curve at T_a (kPa K^{-1}). Situations with a low degree of coupling between the atmosphere and surface (Jarvis & McNaughton 1986) were excluded by only considering values where the decoupling coefficient (Ω) < 0.70 [$\Omega = (s/\gamma + 1)\,(s/\gamma + 1 + g_a/g_s)^{-1}$].

2.5. CO_2 fluxes. A temporal distinction was made between nighttime (F_n) and daytime CO_2 fluxes (F_d). A process-based distinction was made between respiratory (F_r) and assimilatory CO_2 fluxes (F_a). F_n was assumed to exclusively represent an upward F_r. F_d was assumed to represent the sum of a downward F_a and an upward F_r (Ruimy et al. 1995). Instantaneous F_r and F_a were derived from F_d and F_n and used for analysis. Linear regression was done by the least squares technique; non-linear regression analysis followed the iterative Marquardt-Levenberg algorithm (Fox et al. 1994).

2.6. Respiratory CO_2 flux. The dependence of biological activity on temperature has been well established. Lloyd & Taylor (1994) developed a semi-empirical relationship that effectively gives a decrease in activation energy at increasing temperature:

$$F_r = F_{r(0)} \times e^{a_1 \times T_a/[(T_a + 273 - a_2) \times (273 - a_2)]} \quad (1)$$

where $F_{r(0)}$ is the (upward) reference F_r (at 0°C; mg m^{-2} s^{-1}) and a_1 and a_2 are parameters that characterize the temperature response. Eq. (1) was fitted to the F_n measurements in Cabauw on a monthly basis. To account for temporal differences in biomass, the reference F_r was left to vary, but a_1 and a_2 were assumed to be constant (Lloyd & Taylor 1994). To avoid anomalous effects due to twilight, F_n values within 30 min from sunset and before sunrise were excluded from regression.

2.7. Assimilatory CO_2 flux. It was assumed that the relationship between T_a and F_n was equivalent to the relationship between T_a and F_r. F_r was calculated from Eq. (1) as a function of T_a and subtracted from F_d.

The derived F_a values were fitted to R_s using a conventional rectangular hyperbola:

$$F_a = -\varepsilon \times F_{a,mx} \times R_s/(\varepsilon \times R_s + F_{a,mx}) \quad (2)$$

where $F_{a,mx}$ is the asymptotic value of (downward) F_a at saturating irradiance (mg m^{-2} s^{-1}) and ε the slope of the hyperbole at R_s = 0 W m^{-2} (mg J^{-1}).

The effect of T_a and g_s on $F_{a,mx}$ was evaluated. In view of the effect of D on g_s (Leuning 1995), the (apparent) effect of D on $F_{a,mx}$ was also evaluated. The effects were included in $F_{a,mx}$ as multipliers (Eq. 2) as shown in Fig. 1.

The effect of T_a was characterized by the temperatures between which relative $F_{a,mx}$ increases from 0 to 1 (T_0 and T_1). The effect of g_s was characterized by the g_s below which relative $F_{a,mx}$ is less than 1 ($g_{s,i}$) and the reducing effect per unit of g_s (b_g). The effect of D was characterized by the D beyond which relative $F_{a,mx}$ is less than 1 (D_i) and the reducing effect per unit of D (b_D).

2.8. Additional CO_2 sources. Regular traffic occurred on a provincial road at 750 to1500 m distance. At such a distance from the measurement mast, the CO_2 emission from the traffic resulted in a homogeneously mixed increase of the upward F. Indeed, the fitted relationships between short-wave irradiance and F_a did not differ for different wind direction sectors.

Emission by cattle was set at 3.9 kg C d^{-1} for a cow and 2.4 kg C d^{-1} for a young animal (Langeveld et al. 1997). At 1.7 cows ha^{-1} and 0.9 young animals ha^{-1} (farm survey), the total emission amounts to 0.038 mg CO_2 m^{-2} s^{-1}. Due to clustering of cattle, the emission may have been higher and discontinuous in time.

The cattle produced approximately 180 t C yr^{-1} as manure (Langeveld et al. 1997). At a humification coefficient of 0.58 (Kolenbrander 1974), this results in an emission from the manure of 0.006 mg CO_2 m^{-2} s^{-1},

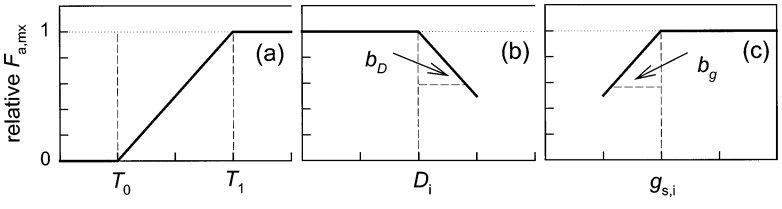

Fig. 1. Asymptotic value of the assimilatory CO_2 flux ($F_{a,mx}$): effect of (a) temperature (T_a), (b) vapour pressure deficit (D), and (c) surface conductance (g_s). b_D and b_g: reducing effects per unit of D and g_s, respectively

which is negligible in comparison to F_r. At the scale of these measurements there is little conceptual difference between manure and soil organic matter.

3. RESULTS

3.1. Respiratory CO_2 flux

Eq. (1) was fitted to F_n and T_a. The fitted parameters a_1 and a_2 were 765 and 180 K, respectively (r^2 = 0.62, n = 2345). Table 1 and Fig. 2 show the monthly values and annual patterns of $F_{r(0)}$. Fig. 3 shows the monthly fitted relationships between T_a and F_n. The annual $F_{r(0)}$ was higher in 1993 (0.103 mg m^{-2} s^{-1}) than in 1994 (0.083 mg m^{-2} s^{-1}).

3.2. Assimilatory CO_2 flux

Eq. (2) was fitted to F_a and R_s. Fig. 4 shows that the fitted yearly $F_{a,mx}$ was higher in 1993 (1.68 mg m^{-2} s^{-1}) than in 1994 (0.99 mg m^{-2} s^{-1}). ε was slightly lower in 1993 (3.4 µg J^{-1}) than in 1994 (3.9 µg J^{-1}).

Table 1 and Fig. 5 show that monthly ε mostly ranged from 4.0 to 5.5 µg J^{-1}, and that the fitted $F_{a,mx}$ ranged from 0.5 to 2.5 mg m^{-2} s^{-1}.

Fig. 2 shows that the monthly levels of $F_{r(0)}$, $F_{a,mx}$, T_a and R_s were lower in 1994 than in 1993. $F_{a,mx}$ and $F_{r(0)}$ were correlated at r = 0.81 (n = 18).

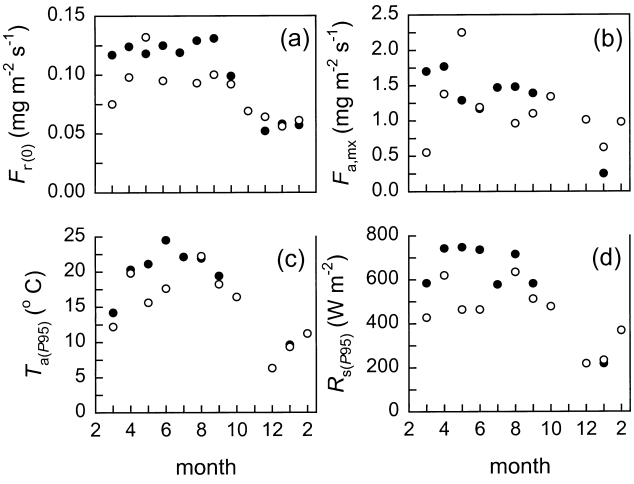

Fig. 2. Annual pattern in 1993 (●) and 1994 (○) of monthly fitted: (a) reference respiratory CO_2 flux ($F_{r(0)}$); (b) asymptotic value of the assimilatory CO_2 flux ($F_{a,mx}$ at optimum T_a); (c) 95 percentile of temperature (T_a); and (d) 95 percentile of short-wave irradiance (R_s)

Inclusion of T_a in $F_{a,mx}$ resulted in a modification of the hyperbola at non-limiting T_a (Table 1, Fig. 6). ε increased to approximately 4.0–7.0 µg J^{-1}. Fitted $F_{a,mx}$ increased in winter and decreased during the rest of the year. Table 1 and Fig. 7a show that the fitted temperature range over which $F_{a,mx}$ responded (T_0 to T_1) coincided with the actual temperature range (represented by the monthly 5 and 95 percentiles of T_a).

Table 1. Regression coefficients ($p < 0.10$) and explained variances (r^2) for respiratory CO_2 flux (F_r) as a function of temperature (T_a) and assimilatory CO_2 flux (F_a) as a function of short-wave irradiance (R_s) and T_a in the wind direction range 195°–250°. p_5, p_{95}: 5 and 95 percentiles of daytime T_a

	$F_r = f(T_a)$			$F_a = f(R_s)$				$F_a = f(R_s,T_a)$					p_5–p_{95}
	n	r^2	$F_{r(0)}$ (mg m^{-2} s^{-1})	n	r^2	$F_{a,mx}$ (mg m^{-2} s^{-1})	ε (µg J^{-1})	r^2	$F_{a,mx}$ (mg m^{-2} s^{-1})	ε (mg J^{-1})	T_0 (°C)	T_1 (°C)	T_a (°C)
Mar 1993	80	0.15	0.117	92	0.82	4.44	2.2	0.86	1.70	3.9		13.1	−0.8–14.2
Apr 1993	58	0.29	0.124	109	0.79	1.78	5.6	0.79	1.77	5.9		16.7	8.2–20.3
May 1993	53	0.22	0.118	155	0.77	1.43	3.8	0.78	1.29	4.8	5.0	15.1	9.7–21.1
Jun 1993	38	0.09	0.125	63	0.72	1.28	5.2	0.76	1.17	6.3	11.5	12.9	10.2–24.5
Jul 1993	133	0.19	0.119	267	0.74	1.53	4.0	0.78	1.47	5.2	7.5	19.7	11.1–22.1
Aug 1993	107	0.17	0.129	200	0.77	1.58	5.6	0.80	1.48	7.2	8.4	18.7	12.4–21.9
Sep 1993	19	0.05	0.131	73	0.55	1.46	7.6	0.61	1.39	8.5	10.7	13.4	12.3–19.4
Jan 1994	331	0.17	0.058	164	0.16	0.17	6.2	0.26	0.25	4.7		5.8	0.9–9.6
Mar 1994	226	0.31	0.075	157	0.57	0.55	5.1	0.57	0.55	5.4		5.9	3.2–12.2
Apr 1994	64	0.48	0.098	151	0.74	1.45	4.3	0.76	1.38	4.7		7.4	1.9–19.8
May 1994	25	0.16	0.132	55	0.92	2.60	4.3	0.93	2.25	5.1	7.0	14.6	7.8–15.6
Jun 1994	63	0.10	0.095	126	0.85	1.19	4.5	0.85	1.19	4.5	9.1	11.9	11.4–17.6
Aug 1994	117	0.05	0.093	185	0.55	0.79	4.1	0.66	0.96	4.8	8.3	20.8	12.8–22.2
Sep 1994	133	0.11	0.100	123	0.70	1.02	3.9	0.71	1.10	4.3		17.7	11.2–18.2
Oct 1994	41	0.22	0.092	40	0.86	1.33	3.6	0.89	1.34	4.2		15.8	5.6–16.4
Dec 1994	123	0.22	0.064	39	0.66	0.51	4.3	0.81		4.3	−4.8		−1.8–6.3
Jan 1995	150	0.23	0.056	97	0.77	0.58	4.2	0.87	0.62	4.3			1.8–9.3
Feb 1995	281	0.18	0.061	217	0.80	0.88	3.8	0.85	0.98	4.9		10.2	4.0–11.2

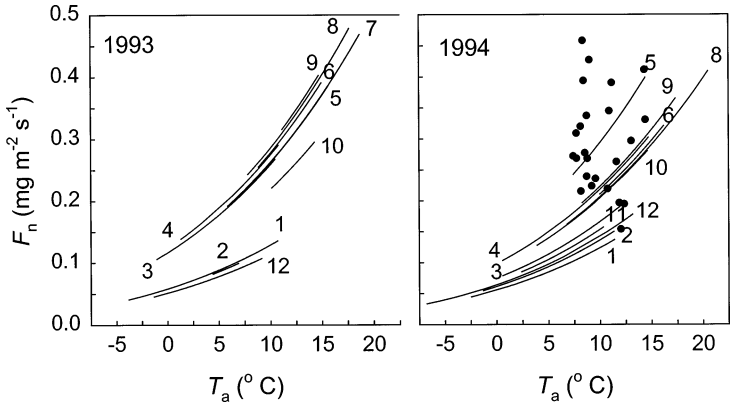

Fig. 3. Monthly fitted relationships between air temperature (T_a) and respiratory CO_2 flux (F_r) in the wind direction range 195°–250°. Actual observations are shown for May 1994

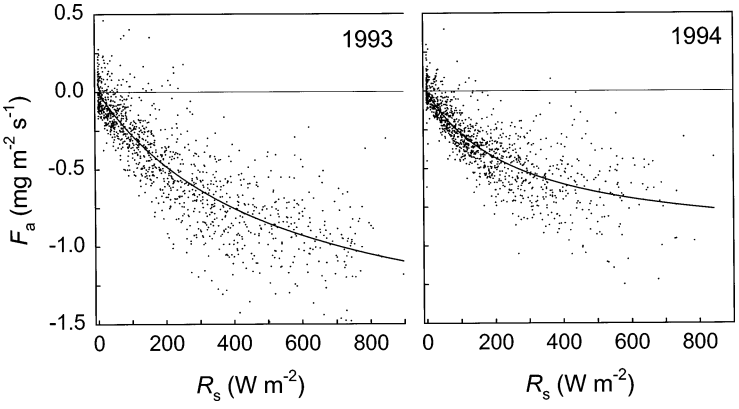

Fig. 4. Assimilatory CO_2 flux (F_a) as a function of short-wave irradiance (R_s) and fitted hyperbolic relationships in 1993 and 1994 in the wind direction range 195°–250°

Inclusion of either D or g_s in $F_{a,mx}$ slightly modified only some hyperbolic relationships at non-limiting levels of D or g_s (Fig. 6). For these, ε decreased and $F_{a,mx}$ increased. Fig. 7b suggests that the effect of D on fitted $F_{a,mx}$ was marginal: the value of D beyond which $F_{a,mx}$ was reduced (D_i) generally coincided with the upper level of the actual range of D (95 percentile of D).

3.3. Diurnal patterns and hysteresis

F_d, F_a, T_a, aerial CO_2 concentration at 1 m height (c_a) and g_s were clustered to monthly average diurnal patterns. Before and after noon responses of these variables to R_s were compared (Fig. 8). August 1993 represents a relatively average summer month, whereas August 1994 represents one of the driest months in the experimental period.

F_d and F_a displayed little hysteresis. In the lower part of the response curve, downward afternoon F were slightly larger than downward before noon F, though within the variation around the curves (not shown). The before noon c_a was up to 30 µmol mol^{-1} higher than the afternoon c_a. Before noon g_s was higher than afternoon g_s during the growing season, and the reverse was true in winter.

4. DISCUSSION

4.1. Respiratory CO_2 fluxes

Fig. 3 shows that part of the year-round response of F_r to T_a was apparent and associated with a correlation between T_a and $F_{r(0)}$—a measure for total biomass and capacity for chemical oxidization. The monthly fit of Eq. (1) shows that short-term variation in F_r could be partly attributed to T_a, albeit not convincingly.

Most of the variation went unexplained. An important source may be the relatively low reliability of micrometeorological measurements at night, resulting in a higher relative variation. Soil moisture (θ) is an additional factor in below-ground respiration (Rochette et al. 1991, Kim et al. 1992, Raich & Schlesinger 1992, Hanson et al. 1993). In peat soils, drainage results in better aeration and often increases below-ground respiration (Raich &

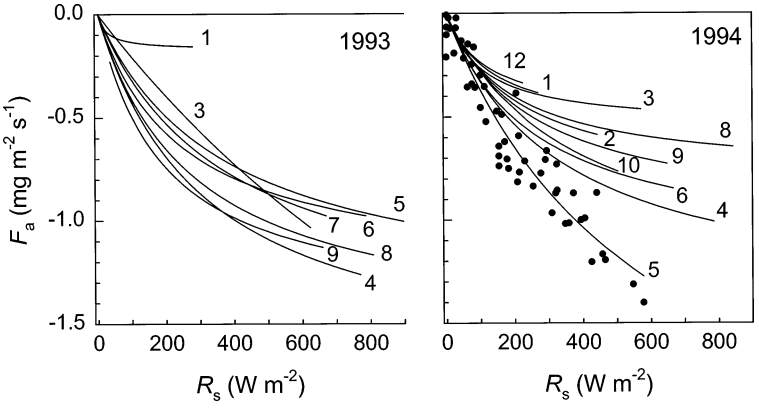

Fig. 5. Monthly fitted relationships between short-wave irradiance (R_s) and assimilatory CO_2 flux (F_a) in the wind direction range 195°–250°. Actual observations are shown for May 1994

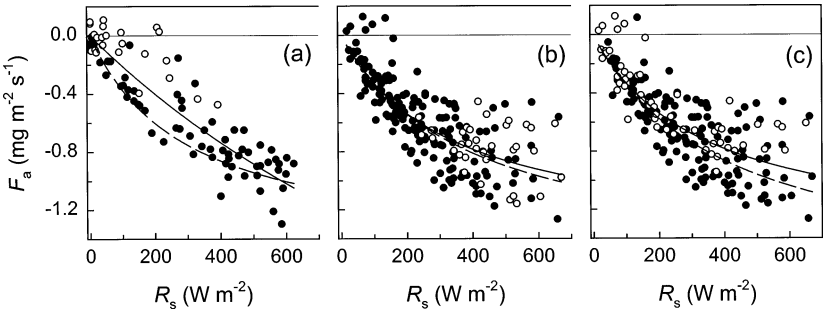

Fig. 6. Assimilatory CO_2 flux (F_a) as a function of short-wave irradiance (R_s). (a) March 1993: T_a > 7.5 (●) and < 7.5°C (○); (b) July 1993: D < 0.75 (●) and > 0.75 kPa (○); (c) July 1993: g_s > 0.75 (●) and < 0.75 cm s^{-1} (○). Curves: average (drawn) and non-limiting T_a, D and g_s (– – –)

Schlesinger 1992, Silvola et al. 1996). The slope of the response curve of F_r to T_a was slightly lower than the one determined by Lloyd & Taylor (1994) for respiration at optimum θ. In this experiment's peat pastures, a low horizontal diffusivity causes a fluctuating groundwater table in the subsoil (Schothorst 1982). This could have caused temporarily suboptimal θ for respiratory activity and added to a heterogeneous response to T_a. Varying contributions from soil organic matter, litter and vegetation to F_r could have resulted in varying ecosystem responses to T_a. The below-ground part in F_r responds to soil temperature, which itself is subject to vertical variation. Rainfall affects soil CO_2 flows by additional dissolution, reduced diffusivity and upward flushes (Rochette et al. 1991).

Generalization of F_n to F_r (Woledge & Parsons 1986) is not undisputed. Robson et al. (1988) argued that dark respiration in grass may be partly suppressed under illumination. But in view of the unknown partial contributions from soil and vegetation to F_r, and the notion that under high irradiance the dark respiration in grass is generally less than 10% of its net photosynthesis (Robson et al. 1988), we assumed the generalization to be acceptable.

Two simpler relationships between T_a and F_r were tested. The variance explained by either a fitted exponential relationship (Q_{10} = 2.3) or a fitted Arrhenius relationship (E = 48 kJ mol^{-1}) was similar to that for Eq. (1).

4.2. Assimilatory CO_2 fluxes

The annual pattern of the asymptotic value of the $F_{a,mx}$ in Fig. 2 was not affected by additional consideration of T_a, D or g_s. The pattern was probably related to shifts in leaf area. The correlation between the $F_{r(0)}$ and $F_{a,mx}$ as well as their temporal patterns (Fig. 2) suggest that both constitute a measure for metabolically active biomass. Their patterns compare well with general patterns of grassland productivity (Corrall & Fenlon 1978). Fung et al. (1987) suggested a proportionality between net primary productivity and the F. Annual differences in $F_{a,mx}$ may be associated with levels of T_a and R_s: low T_a causes a reduced response of the F_a to R_s; low T_a and R_s thus result in a smaller leaf area by the temporal amplification of instantaneous effects.

The positive effect of T_a on $F_{a,mx}$ over the full actual range of T_a (Fig. 7a) is consistent with observations at plant level (Wilson & Cooper 1969, Woledge & Dennis 1982, Woledge & Parsons 1986). Interference of T_a and D often causes an apparent absence of an effect of T_a on CO_2 assimilation (Woledge et al. 1989).

An overestimation of F_r could result in an apparent effect of T_a on $F_{a,mx}$. An overestimation of F_r could result from both the similarity assumption of F_n and F_r (Woledge & Parsons 1986) and an incorrect relationship between T_a and F_n. However, effects of T_a were also found for the net CO_2 flux (F_d). This supports the hypothesis that T_a affected gross canopy CO_2 assimilation over its full range, and not just F_a as an artefact.

Effects of g_s on F_a were not observed, possibly because the range of g_s at

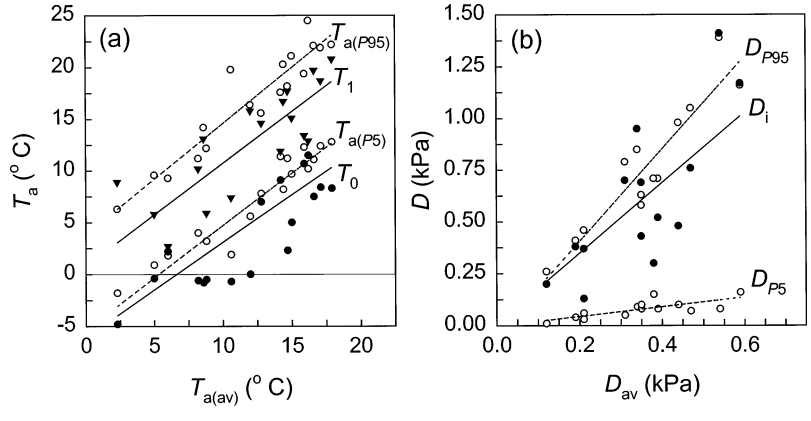

Fig. 7. (a) Monthly 5 and 95 percentiles of daytime T_a (○, ---) as a function of average T_a: monthly T_0 (●) and T_1 (▼); (b) monthly 5 and 95 percentiles of daytime D (○, ---) as a function of average D: monthly D_1 (●). (—) p < 0.10

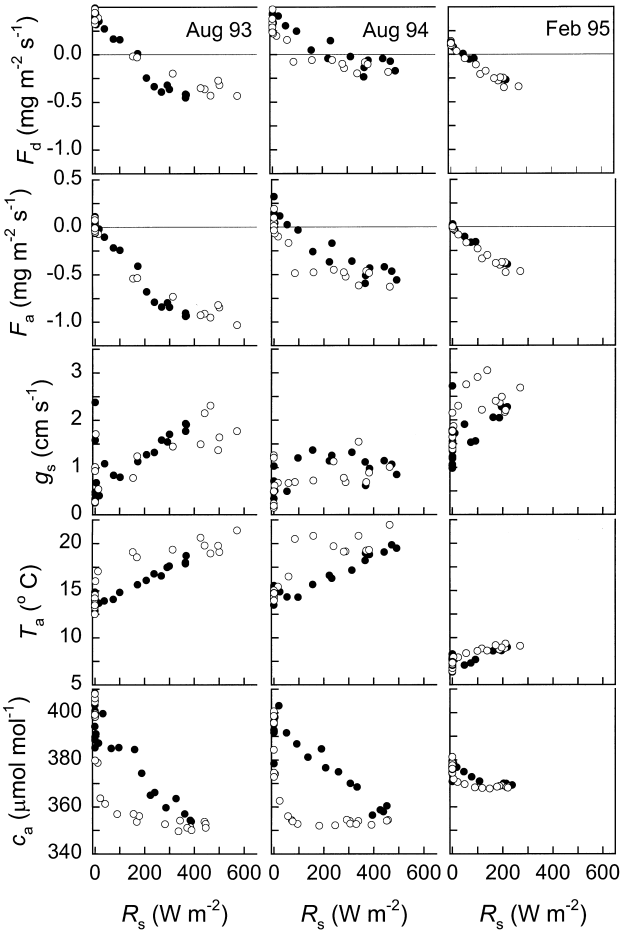

Fig. 8. Average diurnal response to short-wave irradiance (R_s) of the daytime net CO_2 flux (F_d), assimilatory CO_2 flux (F_a), surface conductance (g_s), air temperature (T_a) and aerial CO_2 concentration at 1 m height (c_a) before (●) and after noon (○), in the wind direction range 195°–250°; for each 30 min average n ≥ 3

higher levels of R_s was generally small. Moreover, the relationship between g_s and F_a is an ambiguous one, distinguishing between 2 stages: (1) where g_s follows F_a (Collatz et al. 1991), and (2) where decreasing soil moisture or increasing D decreases g_s (Verma et al. 1986, Woledge et al. 1989, Jarvis 1995). These stages are roughly confined to parts of the response curve: (1) at the full range of R_s (F_a sets g_s); and *(b)* where F_a becomes saturated by irradiance (g_s sets F_a). Low levels of g_s occur at both ends of the response curve, complicating the scheme in Fig. 1c.

D served as a short-cut for g_s (Jarvis 1981, Collatz et al. 1991). It lacks the ambiguity that characterizes g_s, since D correlates with R_s. The response of F_a to D was slightly clearer than for g_s, but a major suppression was not observed. Leuning (1995) considered the effect of D on g_s and photosynthesis, but only above 1 kPa. In our observations D was generally less than 1 to 1.5 kPa.

4.3. Diurnal patterns and hysteresis

The effect of T_a on F_a and the interactions with D and g_s are also illustrated in Fig. 8. The response of the afternoon F to R_s appeared somewhat stronger than of the before noon F. This may indeed be an artefact, since atmospheric conditions change over the day with consequences for the applicability of the aerodynamic theory. But it may also be a genuine response, with low morning temperatures limiting photosynthesis in comparison to the afternoon. An ongoing F_a gradually depleted aerial CO_2 right above the canopy down to its background level around noon; the background CO_2 concentration itself was 350 µmol mol^{-1} in summer and 365 µmol mol^{-1} in winter.

Acknowledgements. This study was partly funded by the National Research Programme on Global Air Pollution and Climate Change (project no. 852062). KNMI provided site facilities and processed the meteorological data. R. Rabbinge commented on the manuscript.

LITERATURE CITED

Anderson DE, Verma SB (1986) Carbon dioxide, water vapor and sensible heat exchanges of a grain sorghum canopy. Boundary Layer Meteorol 34:317–331

Anderson DE, Verma SB, Rosenberg NJ (1984) Eddy correlation measurements of CO_2, latent heat, and sensible heat fluxes over a crop surface. Boundary Layer Meteorol 29: 263–272

Bacastow RB, Keeling CD, Whorf TP (1985) Seasonal amplitude increase in atmospheric CO_2 concentration at Mauna Loa, Hawaii, 1959–1982. J Geophys Res 90D:10529–10540

Baldocchi D (1994) A comparative study of mass and energy exchange rates over a closed C_3 (wheat) and an open C_4 (corn) crop: II. CO_2 exchange and water use efficiency. Agric For Meteorol 67:291–321

Baldocchi DD, Verma SB, Rosenberg NJ (1981) Mass and energy exchanges of a soybean canopy under various environmental regimes. Agron J 73:706–710

Box EO (1988) Estimating the seasonal carbon source-sink geography of a natural, steady-state terrestrial biosphere. J Appl Meteorol 27:1109–1124

Cleveland WS, Freeny AE, Graedel TE (1983) The seasonal component of atmospheric CO_2: information from new approaches to the decomposition of seasonal time series. J Geophys Res 88C:10934–10946

Collatz GJ, Ball JT, Grivet C, Berry JA (1991) Physiological and environmental regulation of stomatal conductance, photosynthesis and transpiration: a model that includes a laminar boundary layer. Agric For Meteorol 54:107–136

Corrall AJ, Fenlon JS (1978) A comparative method for describing the seasonal distribution of production from grasses. J Agric Sci 91:61–67

Dunin FX, Meyer WS, Wong SC, Reyenga W (1989) Seasonal change in water use and carbon assimilation of irrigated wheat. Agric For Meteorol 45:231–250

Fan SC, Wofsy SC, Bakwin PS, Jacob DJ (1990) Atmosphere-biosphere exchange of CO_2 and O_3 in the Central Amazonian forest and the atmosphere. J Geophys Res 95: 16825–16838

Fox E, Kuo J, Tilling L, Ulrich C (1994) SigmaStat user's manual. Jandel Scientific, Erkrath

Fung I, Prentice K, Matthews E, Lerner J, Russell G (1983) Three-dimensional tracer model study of atmospheric CO_2: response to seasonal exchanges with the terrestrial atmosphere. J Geophys Res 88C:1281–1294

Fung IY, Tucker CJ, Prentice KC (1987) Application of advanced very high resolution radiometer vegetation index to study atmosphere-biosphere exchange of CO_2. J Geophys Res 92D:2999–3015

Goudriaan J (1994) Biosphere structure, carbon sequestering potential and the atmospheric ^{14}C carbon record. J Exp Bot 43:1111–1119

Grace J, Lloyd J, McIntyre J, Miranda AC, Meir P, Miranda HS, Nobre C, Moncrieff J, Massheder J, Malhi Y, Wright I, Gash J (1995) Carbon dioxide uptake by an undisturbed tropical rain forest in Southwest Amazonia, 1992 to 1993. Science 270:778–780

Hanson PJ, Wullschleger SD, Bohlman SA, Todd DE (1993) Seasonal and topographic patterns of forest floor CO_2 efflux from an upland oak forest. Tree Physiol 13:1–5

Hensen A, van der Bulk WCM, Vermeulen AT, Wyers GP (1997) CO_2 exchange between grassland and the atmosphere. Report ECN-C-97-032. Netherlands Energy Research Foundation, Petten

Houghton JT, Meira Filho LG, Callander BA, Harris N, Kattenberg A, Maskell K (1996) Climate change 1995: the science of climate change. Cambridge University Press, Cambridge

Hudson RJM, Gherini SA, Goldstein RA (1994) Modeling the global carbon cycle: nitrogen fertilization of the terrestrial biosphere and the 'missing' CO_2 sink. Global Biogeochem Cycles 8:307–333

Jarvis PG (1981) Stomatal conductance, gaseous exchange and transpiration. In: Grace J, Ford ED, Jarvis PG (eds) Plants and their atmospheric environment—the 21st Symposium of The British Ecological Society, Edinburgh, 1979. Blackwell, Oxford, p 175–204

Jarvis PG (1995) The role of temperate trees and forests in CO_2 fixation. Vegetatio 121:157–174

Jarvis PG, McNaughton KG (1986) Stomatal control of transpiration: scaling up from leaf to region. Adv Ecol Res 15: 1–49

Jones HG (1992) Plants and microclimate, 2nd edn. Cambridge University Press, Cambridge

Kaduk J, Heimann M (1996) A prognostic phenology scheme for global terrestrial carbon cycle models. Clim Res 6:1–19

Keeling CD, Chin JFS, Whorf TP (1996) Increased activity of northern vegetation inferred from atmospheric CO_2 measurements. Nature 382:146–149

Kelliher FM, Leuning R, Raupach MR, Schulze ED (1995) Maximum conductances for evaporation from global vegetation types. Agric For Meteorol 73:1–16

Kim J, Verma SB, Clement RJ (1992) Carbon dioxide budget in a temperature grassland ecosystem. J Geophys Res 97D:6057–6063

King AW, Emanuel WR, Wullschleger SD, Post WM (1995) In search of the missing carbon sink: a model of terrestrial biospheric response to land-use change and atmospheric CO_2. Tellus 47B:501–519

Kohlmaier GH, Siré EO, Janececk A, Keeling CD, Piper SC, Revelle R (1989) Modelling the seasonal contribution of a CO_2 fertilization effect of the terrestrial vegetation to the amplitude increase in atmospheric CO_2 at Mauna Loa Observatory. Tellus 41B:487–510

Kolenbrander GJ (1974) Efficiency of organic manure in increasing soil organic matter content. In: Transactions of 10th International Congress for Soil Science, Moscow, Vol 2. International Soil Science Society, Moscow, p 129–136

Langeveld CA, Segers R, Dirks BOM, van den Pol-van Dasselaar A, Velthof GL, Hensen A (1997) Emissions of CO_2, CH_4 and N_2O from pasture on drained peat soils in the Netherlands. Eur J Agron 7:35–42

Leuning R (1995) A critical appraisal of a combined stomatal-photosynthesis model for C_3 plants. Plant Cell Environ 18: 339–355

Lhomme JP (1991) The concept of canopy resistance: historical survey and comparison of different approaches. Agric For Meteorol 54:227–240

Lloyd J, Taylor JA (1994) On the temperature dependence of soil respiration. Funct Ecol 8:315–323

Manabe S, Stouffer RJ, Spelman MJ, Bryan K (1991) Transient responses of a coupled ocean-atmosphere model to gradual changes of atmospheric CO_2. Part I: annual mean response. J Clim 4:785–818

Mascart P, Taconet O, Pinty JP, Ben Mehrez M (1991) Canopy resistance formulation and its effect in mesoscale models: a HAPEX perspective. Agric For Meteorol 54:319–351

McGinn SM, King KM (1990) Simultaneous measurements of heat, water vapour and CO_2 fluxes above alfalfa and maize. Agric For Meteorol 49:331–349

Monteith JL, Unsworth MH (1990) Principles of environmental physics, 2nd edn. Arnold, London

Nemry B, François L, Warnant P, Robinet F, Gérard JC (1996) The seasonality of the CO_2 exchange between the atmosphere and the land biosphere: a study with a global mechanistic vegetation model. J Geophys Res 101D:7111–7125

Raich JW, Schlesinger WH (1992) The global carbon dioxide flux in soil respiration and its relationship to vegetation and climate. Tellus 44B:81–99

Robson MJ, Ryle GJA, Woledge J (1988) The grass plant—its form and function. In: Jones MB, Lazenby A (eds) The grass crop—the physiological basis of production. Chapman and Hall, London, p 27–83

Rochette P, Desjardins RL, Pattey E (1991) Spatial and temporal variability of soil respiration in agricultural fields. Can J Soil Sci 71:189–196

Ruimy A, Jarvis PG, Baldocchi DD, Saugier B (1995) CO_2 fluxes over plant canopies and solar radiation: a review. Adv Ecol Res 26:1–68

Saugier B, Katerji N (1991) Some plant factors controlling evapotranspiration. Agric For Meteorol 54:263–277

Schothorst CJ (1982) Drainage and behaviour of peat soils. In: de Bakker H, van den Berg MW (eds) Proceedings of the symposium on peat lands below sea level. International Institute for Land Reclamation and Improvement, Wageningen, p 130–163

Sellers PJ, Mintz Y, Sud YC, Dalcher A (1986) A Simple Biosphere model (SiB) for use within general circulation models. J Atmos Sci 43:505–531

Silvola J, Alm J, Ahlholm U, Nykänen H, Martikainen PJ (1996) CO_2 fluxes from peat in boreal mires under varying temperature and moisture conditions. J Ecol 84:219–228

Sundquist ET (1993) The global carbon dioxide budget. Science 259:934–941

Tans PP, Fung IY, Takahashi T (1990) Observational constraints on the global atmospheric CO_2 budget. Science 247:1431–1438

Thom AS (1972) Momentum, mass and heat exchange of vegetation. Q J R Meteorol Soc 98:124–134

Thom AS (1975) Momentum, mass and heat exchange of plant communities. In: Monteith JL (ed) Vegetation and the atmosphere, Vol 1. Academic Press, London, p 57–109

Verma SB, Rosenberg NJ (1976) Carbon dioxide concentra-

tion and flux in a large agricultural region of the Great Plains of North America. J Geophys Res 81:399–405

Verma SB, Baldocchi DD, Anderson DE, Matt DR, Clement RJ (1986) Eddy fluxes of CO_2, water vapor, and sensible heat over a deciduous forest. Boundary Layer Meteorol 36: 71–91

Wilson D, Cooper JP (1969) Effect of temperature during growth on leaf anatomy and subsequent light-saturated photosynthesis among contrasting *Lolium* genotypes. New Phytol 68:1115–1123

Woledge J, Dennis WD (1982) The effect of temperature on photosynthesis of ryegrass and white clover leaves. Ann Bot 50:25–35

Woledge J, Parsons AJ (1986) The effect of temperature on the photosynthesis of ryegrass canopies. Ann Bot 57: 487–497

Woledge J, Bunce JA, Tewson V (1989) The effect of air humidity on photosynthesis of ryegrass and white clover at three temperatures. Ann Bot 63:271–279

Wolf J, Janssen LHJM (1991) Effects of changing land use in the Netherlands on net carbon fixation. Neth J Agric Sci 39:237–246

Editorial responsibility: Gerd Esser, Gießen, Germany

Submitted: February 27, 1998; Accepted: June 8, 1999
Proofs received from author(s): August 30, 1999